

# A Novel Mouse Model of Vascular Cognitive Impairment – A Diffusional Kurtosis Imaging Study

Edward S Hui<sup>1</sup> and Andy Y Shih<sup>2</sup>

<sup>1</sup>The University of Hong Kong, Pokfulam, Hong Kong, Hong Kong, <sup>2</sup>Medical University of South Carolina, Charleston, South Carolina, United States

**Purpose** Cerebral small vessel disease (SVD) refers to vascular pathology that involves small arteries, arterioles, capillaries and small veins<sup>1</sup> of the brain. It is frequently found in patients with dementia or Alzheimer's disease<sup>1</sup>, and is strongly correlated with cognitive impairment<sup>2</sup>. The exact pathological mechanism underlying cognitive impairment remains elusive, yet cerebral microinfarction are believed to be the most plausible vascular pathology<sup>2</sup>. Because of their small size (0.2 – 2.9mm), microinfarcts are often undetected under conventional human MRI<sup>1,2</sup>. A recent study, nonetheless, demonstrates that they can be detected by high-resolution 7.0T MRI<sup>1</sup>. As such, it is imperative to improve the detection of microinfarcts, thereby allowing *in vivo* characterization of the evolution of neuropathology underlying SVD. The *objective* of this study is to investigate the change in brain microstructure along the course of microinfarction using a novel mouse model<sup>3</sup> and diffusional kurtosis imaging<sup>4</sup>.

**Methods** Microinfarction Surgery was performed on 3 mice (20-25g). To obtain optical clarity to the cerebral cortex for the purpose of photothrombotic occlusion of blood vessel, a non-invasive thin-skulled cranial window<sup>5</sup> was generated, which avoids surgically-induced inflammation. The vasculature was labeled by IV injection of Texas Red-dextran and visualized under two-photon microscopy<sup>6</sup>. A single penetrating arteriole was photothrombotically occluded with a focused green laser (wavelength: 920–950nm) and circulating photosensitizer, Rose Bengal, to induce microinfarction<sup>7</sup>. 3 microinfarcts (diameter: 0.1–0.6mm) were induced for each animal. **MRI** *In vivo* experiments were performed on a 7T Bruker scanner at 6 hours (6h), 1 (1d), 3 (3d), 7 (7d) and 14 (14d) days after microinfarction. Diffusion-weighted images (DWIs) were acquired with a 4-shot SE-EPI sequence along 64 diffusion encoding directions and 3 b-values (0, 1000, 2000 s/mm<sup>2</sup>) using:  $\delta/\Delta/\text{TR}/\text{TE}=5/18/3000/31\text{ms}$ , TH=0.5mm, matrix=128x128, FOV=20x20mm<sup>2</sup>, NEX=2. ROIs of microinfarct were drawn on the average of all DWIs with b-value of 2000s/mm<sup>2</sup> (mDWI<sub>2000</sub>) acquired at 6h, and were subsequently applied to similar location for other time points.

**Results and Discussion** **Fig.1** shows the T2-weighted image (T2W), mDWI<sub>2000</sub>, MD and MK maps of a mouse at 6h, 1d, 3d, 7d post-microinfarction. The 3 microinfarcts varied in sizes, depending on the pre-occlusion flux of red blood cells through the targeted vessel. At 6h, MD reduced and MK increased (similar to ischemic stroke<sup>8</sup>), and the change peaked at 1d post-microinfarction. Notice 2 of the microinfarcts (indicated by red arrows in **Fig.1**) degenerated in a much quicker pace than that caudal to them. The MK of all microinfarcts remained elevated up to 3d amid pseudonormalization of MD of those indicated by red arrow. The observation of which is corroborated by the ROI analysis in **Fig. 2**. It is noteworthy that the MK of microinfarct pseudonormalized at an earlier time point than that of ischemic stroke which remained elevated up to 7d post-stroke<sup>8</sup>, suggesting the difference in the temporal dynamics of the

underlying pathological processes between the two neurological disorders. In summary, we have developed a novel mouse model of cortical microinfarcts, a hallmark of SVD and vascular dementia. This model enables production of microinfarcts of varied size and location with high fidelity. Future studies will investigate the pathophysiological mechanism underlying the evolution of microinfarction using *in vivo* MRI and two-photon microscopy.

**References** 1. van Veluw SJ, et al. *JCBFM*. 2013;33(3):322-329. 2. Smith EE, Set al. *Lancet Neurol*. 2012;11(3):272-282. 3. Shih AY, et al. *Nat Neurosci*. 2013;16(1):55-63. 4. Jensen JH, et al. *MRM*. 2005;53(6):1432-1440. 5. Drew PJ, et al. *Nat Methods*. 2010;7:981-984. 6. Shih AY, et al. *JCBFM*. 2012;32(7):1277-1309. 7. Shih AY, et al. New York: Cold Spring Harbor Laboratory Press; 2011. 8. Hui ES, et al. *Brain Res*. 2012;1451:100-109.

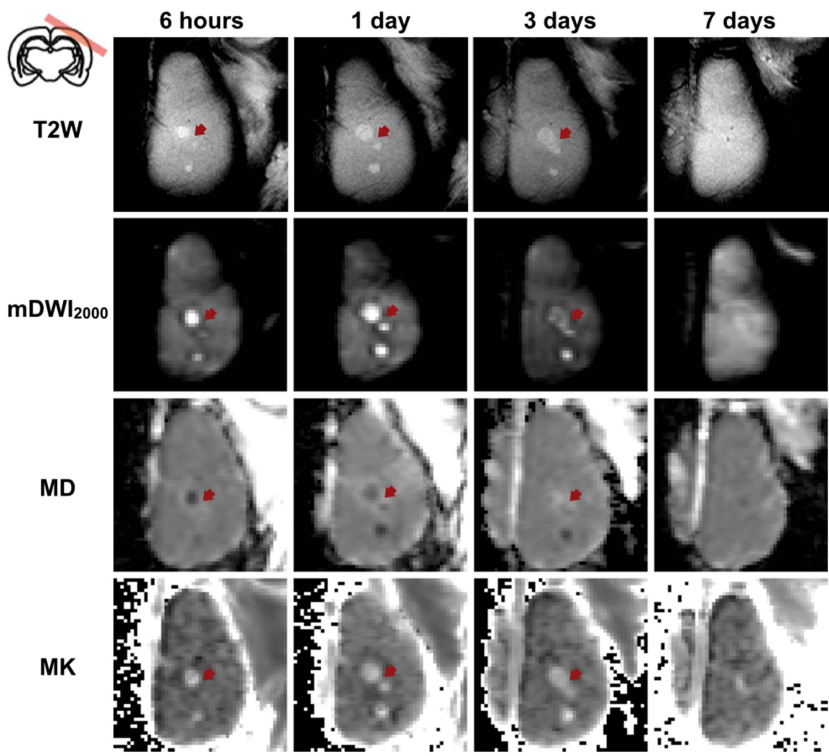
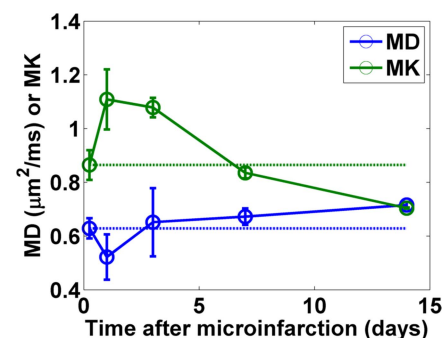


**Fig.1.** Representative mouse at 6 hours, 1, 3 and 7 days after microinfarction. 3 microinfarcts were induced. (a) T2-weighted images (T2W), (b) average of all DWIs with b-value of 2000 s/mm<sup>2</sup> (mDWI<sub>2000</sub>), (c) mean diffusivity (MD), and (d) mean kurtosis (MK) maps. Scale for MD: 0 – 1.5 $\mu\text{m}^2/\text{ms}$ ; MK: 0 – 1.5.

**Fig.2.** ROI measurements (mean  $\pm$  standard deviation) of MD and MK in all microinfarcts of the 3 mice.